CONFERENCE PRE-PRINT

INTEGRATED MODELLING ACTIVITIES IN SUPPORT OF THE ITER RE-BASELINE

M. SCHNEIDER
ITER Organization, St-Paul Lez Durance, France
Email: mireille.schneider@iter.org

J. ARTOLA[1], X. BONNIN[1], M. DUBROV[1], Y. GRIBOV[1], W. HELOU[1], O. HOENEN[1], S.H. KIM[1], F. KOECHL[1], S. KORVING[1], A. LOARTE[1], E. LERCHE[2], S.D. PINCHES[1], R.A. PITTS[1], A.R. POLEVOI[1], M. PREYNAS[1], A. PSHENOV[1], N. SCHWARZ[1], J. STOBER[3], P. VINCENZI[4,5], T. WAUTERS[1]

[1] ITER Organization, St. Paul-lez-Durance Cedex, France,
[2] ERM/KMS, Brussels, Belgium
[3] Max-Planck-Institut für Plasmaphysik, Garching, Germany
[4] Consorzio RFX, Padova, Italy
[5]Institute for Plasma Science and Technology, Nation. Res. Council, 35127 Padova, Italy

Abstract

The new ITER baseline originates from the change of First Wall (FW) material from beryllium (Be) to tungsten (W), implying an adjustment of the plant system configuration and of the various phases of the ITER Research Plan (IRP). This re-baseline has largely been guided by modelling activities supported by the Integrated Modelling and Analysis Suite (IMAS), associated, whenever possible, with validation on currently operating devices. The new baseline will stage the installation of some components (FW, heating systems, etc.) and adapt the wall conditioning techniques, heating mix, and operation scenarios, to overcome the increase of W source and the constraints related to the ITER neutron budget. This paper gives an insight into the modelling tools and analyses which supported the new baseline design, together with the overall international strategy for guidance of Integrated Modelling (IM) activities towards successful ITER operation.

1. INTRODUCTION

The IRP and its recent re-baseline [1,2] have been extensively supported by IM activities based on tools continuously developed by physicists and scenario experts over the last few decades to help optimize the path towards achieving the ITER mission goals. To build the ITER IM platform, the ITER Organization (IO) has pushed the international fusion community towards adopting the standard offered by the IMAS integrated modelling suite [3] to foster collaboration among ITER members. Hence, for the last decade, IMAS has been guiding modellers towards working in a collaborative environment through the provision of standard tools, encouraging experts to design IM suites for worldwide usage. This development has been driven not only by the necessity to build a robust and validated modelling platform for future ITER operation, but also by the continuous need to address fundamental physics issues in view of finalizing the designs of key systems and of the IRP, making this development goal-oriented. One of these goals has been to address the questions related to the adjustment of the ITER staged approach for the new baseline, which is the essence of this paper. Focusing on short-term objectives is the so-called agile approach, meant to be iterative and collaborative, providing adequate initial results subsequently refined with the evolution of models and computational capabilities. Such a community-based approach is enhanced by the recent IO strategy for the promotion of open-source software and open-access to the modelling tools upon which the IMAS suite is built.

2. THE ITER NEW BASELINE

The change of FW material from Be to W [4] necessitated modifications to the configuration of the ITER tokamak and its ancillary systems [5,6]. Since the W FW brings an extra W source to the plasma, radiated power losses increase, which reduces the H-mode operational range and, if uncontrolled, may lead to radiative collapse. Such risks have been assessed both via extrapolation from today's experiments, and through simulations using the IM tools currently available within the community. The current paper focuses on the modelling aspects which have been key in adapting the IRP to minimize the risks associated with the increased W source and to optimise the plant system configuration to ensure that ITER fulfils its mission goals. This has led to the following, three-staged new baseline approach, for which some of the rationale is presented in the next sections:

— **Start of Research Operation (SRO)**: a temporary, inertially cooled FW will be installed for this phase, to minimise the risks to machine integrity during the commissioning of protection and plant systems. The Heating and Current Drive (H&CD) mix will consist of 40 MW of Electron Cyclotron Heating (ECH) and

10 MW of Ion Cyclotron Heating (ICH). The main purposes of this phase are to demonstrate H-mode operation in deuterium (D) and operation to nominal magnetic energy in hydrogen (H), i.e. at 15 MA / 5.3 T.

— **DT-1**: in this phase, the final water-cooled FW will be installed, together with 60-67 MW ECH, 10-20 MW ICH (depending on strategic choices for H&CD upgrades made during SRO), and 33 MW Neutral Beam Injection (NBI) heating. The main goals of DT-1 are to demonstrate a fusion gain $Q \geq 10$ and a fusion power $P_{fus} = 500$ MW for a duration of 300-500 s within a neutron budget of $3.5 \cdot 10^{25}$, equivalent to 1% of the lifetime fluence.

— **DT-2**: this phase aims to demonstrate routine operation at $Q \geq 10$, together with long pulse and steady-state operation at $Q \geq 5$ for 1000-3000 s, within the total ITER neutron budget of $3 \cdot 10^{27}$. To make this possible, an upgrade of the NBI power to 49.5 MW is foreseen (addition of a 3rd NBI source).

3. MODELLING SUPPORT TO BUILD THE ITER NEW BASELINE

The main guidance for the new ITER new baseline comes from observations on present tokamaks. However, for these results to be extrapolated to ITER operation, it is essential to understand the underlying physics processes through appropriate theory and modelling support. These modelling activities cover the following topics:

- **W source and transport in L-mode and H-mode plasmas:** modelling studies have shown that W transport differs between present devices and ITER for L-mode and H-mode plasmas, as described in Section 3.1.
- **H&CD sources and their impact on W source, transport, and MHD stability:** present experiments indicate that the penetration of W to the core plasma may cause radiative collapse [7] which requires central plasma heating to expel W, as explained in Section 3.2.
- **Disruption loads and mitigation:** the new baseline includes a robust commissioning plan to assess disruption loads and test their mitigation strategy as explained in Section 3.3.

In an ideal world, such studies are supported by self-consistent IM of the wall-SOL-pedestal-core regions, including the full dynamics of temperature T_e, density n_e, rotation, and current. This is, however, not yet possible. A comprehensive review of the state-of-the-art of international IM activities towards ITER operation is made in [8]. For ITER, the workhorse of plasma modelling is the JINTRAC [9] transport suite of codes upon which the High-Fidelity Plasma Simulator (HFPS) is built, as thoroughly described in [10]. Other tools are being developed in the context of the ITER IM platform evolution, but since they were not directly used in support of the new baseline, they are not discussed further here. The IM tools used to support the steps and strategy for the ITER new baseline development are listed in Figure 1. This modelling helps to ensure that ITER fulfils its mission goals with the most effective mitigation of operational risks to the integrity of the machine and its plant systems.

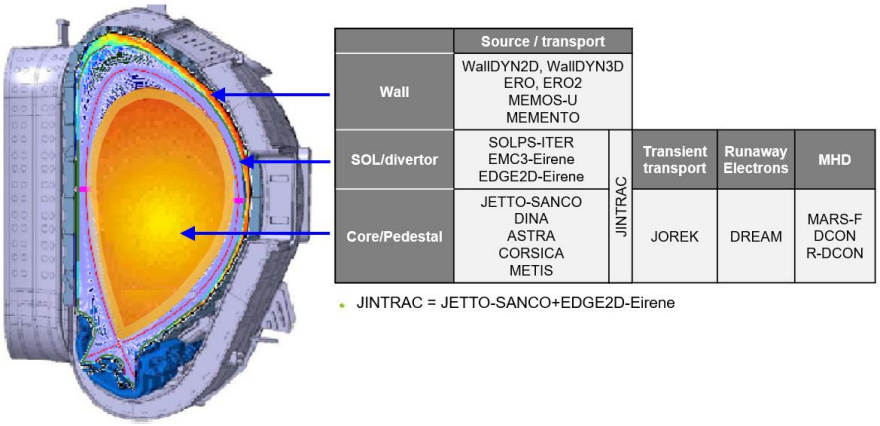

Figure 1 – List of simulation codes used for wall, divertor, SOL (scrape-off-layer), pedestal and core modelling to support the development of the new ITER baseline.

3.1. Effect of W source and transport in L-mode and H-mode plasmas

The gross W source from the wall represents ~10-20% of the gross divertor W source, but its penetration to the core is one order of magnitude higher for the main chamber source compared to that from the divertor. This is due to the lower W prompt redeposition rate and lower SOL W screening for the wall source. The result is a similar contribution from both the wall and divertor sources. The core plasma W contamination from wall to core is determined by transport effects from the wall to the separatrix, and then through the plasma pedestal and core. In the SOL, W transport is assumed to be purely anomalous while in the core it is determined by the competition of anomalous and neoclassical transport. For most ITER plasma conditions, W anomalous transport tends to dominate diffusion in the core (except in some L-mode conditions) and the pedestal while convection is dominated by neoclassical transport in the pedestal and this regulates the physics of W accumulation in ITER plasmas. In

addition, there is the issue of local power balance when, due to an excessive W concentration, the radiative power losses from W on a given flux surface exceed the local heat flux from H&CD sources, that can lead to electron temperature collapse. Such effects are modelled by IM transport suites of codes: edge transport solvers like SOLPS-ITER [11,12] focus on the wall and SOL regions, while core(-edge) transport solvers such as JINTRAC focus on the pedestal and core areas, with an option to extend to the SOL region when coupled to the EDGE2D-Eirene model, as illustrated in Figure 1 [13,14].

3.1.1. Modelling W source and transport in L-mode plasmas

Self-consistent modelling of plasma-wall interactions, transport, and magnetic control is not yet available for accurate simulation of the rather dynamic limiter plasma start-up. Hence, a combination of SOLPS-ITER, including W sputtering and transport but assuming zero prompt re-deposition, and DINA simulations has been used instead: for the limiter phase, the W source and transport is calculated by SOLPS-ITER, to calibrate the W source model embedded in the DINA solver [15], i.e. to introduce a correction factor to the mean energy of ions impinging on the wall which takes into account the difference between the edge temperature $T_{e,LCFS}$ (where DINA simulation grid ends) and the erosion area, as well as a factor representing the screening of eroded neutral W by the SOL plasma [5]. Following X-point formation, DINA uses a prescribed W concentration adjusted according to JINTRAC modelling which, when being run in "COCONUT mode", includes realistic W source calculations from the divertor and main wall (with an ad-hoc source) interactions, i.e. with core-edge transport coupling using JETTO-SANCO [16,17] coupled to EDGE2D-Eirene. In these JINTRAC simulations, TGLF-SAT2 [18] was used for turbulent transport together with NEO [19] for neoclassical transport [20].

Transport in L-mode plasmas can be described as follows:

- On current devices, due to the lower confinement time, the higher core and edge particle transport (no edge transport barrier), and the low power levels, there is reduced W core accumulation compared to H-mode.
- On ITER, despite the low confinement time in L-mode, W accumulation may be significant, arising from neoclassical transport or when W radiative losses are locally higher than the electron heat source, causing possible radiative collapse [7,21].

In the new baseline, one of the main concerns with the W FW is the **higher risk for radiative collapse during the plasma startup and early ramp-up phase**. In these phases, the SOL temperature is sufficient for W sputtering due to the impact of low-Z impurities (principally oxygen). In ITER limiter plasmas, core turbulent and neoclassical W fluxes are comparable, and since W can reach the confined plasma much more readily than in diverted plasmas, the core W concentration increases quickly as soon as the W sputtering starts and the core radiation increases. However, a self-regulation mechanism [5,22] between the plasma and the wall induces a saturation of the W core concentration, leading to thermal stabilization [23]: the initial W release generates radiative losses which reduce $T_{e,LCFS}$, thus reducing the W sputtered influx. The challenge is to pass through this early phase and reach higher plasma current (I_p) without radiative collapse, and this is achieved by the use of **central ECH**. The effect of central ECH on W accumulation in ITER limiter plasmas has been investigated with GRAY [24] for ECH inside the JINTRAC suite, by performing a scan of poloidal steering angle to modify the radial location of ECH/ECCD [5]. This study indicated that ECH should be within $\rho < 0.3$ for efficient absorption, T_e rise and W removal. In contrast, off-axis ECH reduces core turbulent W transport and increases inwards neoclassical W transport, leading to core W accumulation which increases radiation losses in the centre, yielding a hollow core T_e profile provoking a radiative collapse. Passing through the early limiter phase without radiative collapse can also be helped with careful **n_e tailoring** as described further below. Another method is to **inject low-Z impurity** to mitigate W sputtering effects in a controlled way, as demonstrated on WEST [25].

The effect of the W wall has been assessed on ITER using SOLPS-ITER, DINA, and JINTRAC for the simulation of a complete discharge from breakdown to plasma termination. The operational range in L-mode was investigated for various levels of W wall influxes, within 10-20% of the W divertor source, varying n_e and ECH during the current ramp-up of a 15 MA / 5.3 T scenario, as summarised in Table 1, together with the resulting W wall source and associated amount of radiated power. To be conservative, no W prompt redeposition and no neon (Ne) injection for divertor power dissipation have been assumed. This modelling has shown that for these conservative assumptions, n_e should be increased to 0.5 n_{GW} at high I_p to reduce the W source and keep the level of radiated power below 40%. Under these conditions, the divertor power fluxes remain below 10 MW/m^2. The elevated tolerance to high W wall source at low I_p and n_e is due to central ECH which increases T_{e0} (≥ 10 keV) hence reduces the W radiation efficiency: in other words, with ECH and low n_e high W concentration leads to moderate radiated power. To assess the validity of these results, JINTRAC requires further benchmarking against present experiments, including W production and transport.

TABLE 1. ECH and fraction of Greenwald density n_{GW} during ramp-up of a 15 MA / 5.3 T L-mode scenario simulated by JINTRAC and confirmed by DINA [5], with resulting W wall source and radiated power.

I_p [MA]	ECH [MW]	n_{GW}[%]	W wall source	P_{rad}
5	5	30	$3-4\cdot10^{-5}$	< 40%
10	10	30	$3-4\cdot10^{-5}$	< 40%
15	40	50	$1-2\cdot10^{-5}$	< 40%

3.1.2. Modelling W source and transport in ELM-free H-mode plasmas

As already mentioned, integrated transport suites like JINTRAC simulate core-edge plasmas, and, as far as possible, plasma-wall interactions. For the latter, in diverted plasmas, JINTRAC has no realistic means by which to calculate the W wall source since the EDGE2D-Eirene simulation grid is restricted to the first field line which intercepts the wall starting from the divertor area. This means that the W wall source must be provided externally. In H-mode plasmas at $I_p \geq 7.5$ MA, ELMs must be suppressed to avoid melting the W divertor monoblock toroidal gap edges and then, at still higher currents, the top surfaces [26]. For such scenarios, ELMs are therefore assumed not to contribute to the overall W wall source which is generated by the incident stationary plasma ion flux, including impurities, and hydrogenic charge-exchange neutral (CXN) wall fluxes. For the re-baseline studies, this source has so far been estimated primarily using the 2D version of WallDYN [27] which estimates the W wall influx and its penetration up to the near-SOL region [28], from where JINTRAC can take over. Estimates have been performed for a high Ne seeding case (used for divertor detachment control) with various assumptions for far-SOL parameters and transport. These simulations indicate that the dominant mechanism for W production is Ne sputtering and the consequent W self-sputtering. Sputtering induced by fuel CXN wall fluxes is negligible in comparison. WallDYN provides a W ion density at the last numerical grid surface in the JINTRAC mesh and this is then used by JINTRAC to set the density boundary condition at the grid edge. While the SOL transport is rather uncertain and an effective diffusive transport is assumed, both experiments and modelling indicate that the W transport in the H-mode pedestal can be described by neoclassical transport, in particular the convective transport (or pinch). In H-mode pedestals, the direction and amplitude of neoclassical pinch is determined by the n_i and T_i gradients, characterised by the n_i and T_i scale lengths, $L_n = n/\nabla n$ and $L_T = T/\nabla T$:

- When $\left|\frac{R}{L_n}\right| > \left|\frac{R}{2L_T}\right|$, i.e. when n_i gradients are larger than T_i gradients, as is the case on current devices, the **neoclassical pinch is dominant and inwards**, which increases the impurity density from the separatrix to the pedestal, inducing W accumulation in the core plasma.
- When $\left|\frac{R}{L_n}\right| < \left|\frac{R}{2L_T}\right|$, the **neoclassical pinch is outwards**, leading to an expulsion of W from the edge to the separatrix. This is the case for ITER and JET high T_i experiments [29,30], leading to edge W screening.

The same physics applies to the core. In the case of ITER, turbulent transport is dominant over neoclassical transport, leading to relatively flat W profiles [20]. For high Q ITER H-mode plasmas, these effects have been simulated with JINTRAC, indicating no core W accumulation, in agreement with the modelling from [7,20]. In such plasmas, there is no core plasma radiative collapse as such but an edge power deficit leading to the loss of H-mode confinement. Such differences in the dominant W transport between present devices and ITER make simple extrapolations from today's experiments to ITER unreliable and emphasize the importance of self-consistent, integrated modelling of core-edge transport to predict the performance of ITER plasmas.

Core transport in JINTRAC is described either by the EDWM [31] or TGLF-SAT2 [18] models for turbulent transport and NEO for neoclassical transport. ELMs are assumed suppressed by describing the pedestal transport with the continuous ELM model [32] which adjusts transport coefficients to achieve the ideal MHD pressure limit. These simulations are shown in Figure 2, which indicates that $Q \geq 10$ can be maintained for most of the W far-SOL densities estimated with WallDYN (in which the W far-SOL transport is assumed to be turbulent), while for the largest values an increase of the additional heating level to 70 MW is required to compensate the large W radiation and Q decreases to ~7-8.

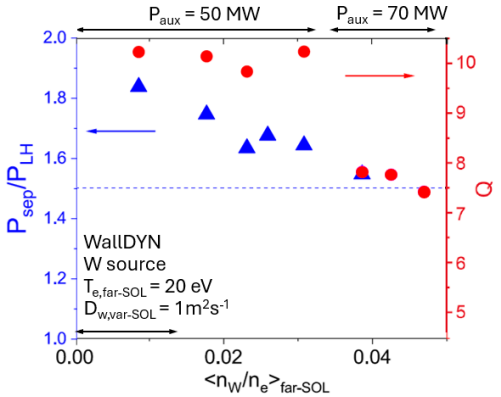

Figure 2 - JINTRAC modelled Q using TGLF-SAT2 (red points) and margin of edge power flow above the L-H transition (blue triangles) vs. average far-SOL W density compared to predictions from WallDYN for 15 MA/5.3 T DT plasmas with additional power heating levels of 50 MW (Q ≥10).

3.1.3. Modelling W source and transport in ELMy H-mode plasmas

The W source can be dominated by ELMs if $T_{e,LCFS}$ is low or, for the wall source, if the plasma-wall distance is large [33,34]. As highlighted earlier, avoidance of ELM transients is important as I_p is raised in the Research Plan. For this reason, SRO H-mode operation (in deuterium plasma) will start only at 5 MA to ensure no melting of divertor monoblock toroidal gaps [26,35]. Only when ELM control is proven effective, will I_p be increased to 7.5 MA. IM studies have been carried out to define SRO achievable H-mode conditions with appropriate ELM control. Two approaches have been adopted in the modelling:

- **ELM-averaged approach:**
  - ***W source***: the gross divertor W source due to ELMs is evaluated using SOLPS simulations [36] and the equivalent W influx to the plasma is calculated as the sum of the effective divertor source including prompt redeposition and the wall source assumed to be ~10% of the W divertor source. Various levels of edge power flow levels and fractions of divertor W prompt redeposition (>95%) during ELMs have been considered, showing that for large W wall sources and low ELM frequencies, the W influx significantly degrades the H-mode performance, further justifying the need for robust ELM control beyond that required for divertor protection.
  - ***W transport*****:** the resulting W influx is then injected into JINTRAC, and the consequence on H-mode performance is simulated using this ELM-averaged W influx with the continuous ELM model to adjust pedestal transport coefficients and obtain the pressure predicted by ideal MHD modelling. SRO H-modes are found to be resilient to W wall influxes due to the W screening at the pedestal from neoclassical transport effects, and to the high core T_{e0} (> 10 keV) ensured by central ECH, leading to a core radiated power $P_{rad} < 10$ MW, even for a W concentration $C_w \sim 10^{-4}$ in 5 MA H-mode plasmas.

- **Full ELM-resolved simulations**: ELM-resolved JINTRAC simulations of the effective core W plasma influx from the divertor are performed and its magnitude simply doubled as a proxy describing the W wall source. The results indicate that for SRO 5 MA H-mode plasmas at 0.5 n_{GW} with 40 MW of central ECH, and assuming 80% of divertor prompt redeposition, a low core radiated power (~18%) is achieved, in agreement with the time-averaged simulations above. However, instantaneous radiative power losses during ELMs are a concern because they are much larger (~15 MW), and can trigger H-L transitions, which again confirms the need for robust ELM control schemes in SRO.

3.1.4. Modelling in support of ELM control strategies

Small/no ELM plasmas are essential to limit the W influx, and access to these regimes will be ensured by control schemes supported by 27 ELM control coils and power supplies, and 4 pellet injectors for **ELM-pacing**, to trigger ELMs with a frequency up to 60 Hz in SRO. However, increasing the ELM frequency would not be sufficient to limit the core W density when pedestal screening is at work. If the W transport is inwards and W profiles in the pedestal are peaked, as in present machines, ELMs provide an efficient W exhaust. On the contrary, if W screening dominates and W density profiles are hollow in the pedestal, ELMs produce an inwards W flux, increasing the core W concentration [36,37] as confirmed in JET [29,30]. Hence, once again ELMs should be suppressed or strongly mitigated both for W density control and divertor ELM power flux control.

Another mitigation strategy based on **high clearance** H-mode plasmas is foreseen in SRO to develop the initial scenarios; this consists in increasing the overall plasma-wall distance or increasing the distance to the outer wall separatrix only, since ELMs are key drivers for the W wall source and their largest effect is on the LFS. However, such modifications degrade the plasma vertical stability (VS) which necessitates more control from in-vessel VS coils for very large clearances. A solution is to reduce the plasma elongation and triangularity, but at the expense of lowering the pedestal pressure, reducing the screening effect and plasma performance, unless n_e is adjusted, but is viable for SRO. Such a strategy has been supported by resistive MHD linear modelling, using the MARS-F code [38], to simulate ELM control with 3D fields using ELM coils and increased wall clearance [39], indicating that ELMs can be equally well mitigated/suppressed with an outer gap wall clearance of 45 cm compared to the normal clearance (15 cm), by doubling the current in the ELM coils, which remains far from the current coil limit for SRO 5 MA H-mode plasmas. Modelling results also show that I_p can be slightly reduced to adjust q_{95}, maximising the X-point displacement for optimal ELM mitigation.

A caveat to this control scheme arises from recent 3D field modelling applied to ELM control [40], which shows that induced **3D fields may have a direct effect on W edge neoclassical transport.** When the neoclassical pinch is inwards (as on today's devices), 3D structures increase the outwards W transport. When the W is screened at the edge (as on ITER), 3D structures decrease the outwards W transport, leading to W core accumulation. Such results indicate that a balance is needed between ELM control and the preservation of the W pedestal screening when 3D fields are applied.

The overall strategy for ELM control is built upon a combination of experimental and IM activities to extrapolate to ITER. So far, no integrated model can perform a full simulation including a description of the divertor and wall sources. Improvements are needed to better describe the W transport from the source to the plasma core. These gaps are compensated by experimental observations to quantify the impact of ELM and inter-ELM periods on W sources and associated edge W transport. Experiments on present devices are again key to validate the models and assumptions made to predict SRO scenarios.

3.2. H&CD sources and their impact on W source, transport, and MHD stability

3.2.1. Modelling the effect of ECH and ICH on W core concentration and possible radiative collapse

To fulfil the needs for robust and sustainable H-mode access ($P_{sep} \geq 1.5\ P_{LH}$ with P_{LH} from Martin's scaling law [41] combined with isotopic effects for T, i.e. $P_{LH,DT} = 0.8\ P_{LH,DD}$ [42,43]), ~50 MW is required for H-modes in SRO D plasmas(at 5 MA and 7.5 MA, B=2.65T, $n \leq 0.85 n_{GW}$), and ~100 MW for H-mode above 10 MA in D plasmas (in DT-1 and beyond at B=5.3T, $n \leq 0.85 n_{GW}$). For DT-2, more current drive is needed for hybrid and non-inductive operation, which, since NBI is the main source of external current drive, relies on an upgrade of the NBI power from 33 to 49.5 MW. The margin on the L-H power threshold is expected to compensate for the enhanced core radiation which should not exceed ~50% to ensure robust H-mode operation [1]. For high W concentrations ($C_W > 10^{-5}$), such performance requires central plasma heating to expel W from the core. For this reason, the new baseline includes more ECH power, and the magnetic fields are restricted to half field (2.65T) and full field (5.3T) to ensure that it remains central. ECH is favoured over ICH since ICH may induce additional W influxes due its interaction with the W FW [44]. However, such effects are expected to remain small with appropriate antenna design and operation [47]. Several modelling studies have been performed to predict and successfully minimize the impact of ICH on W sources and transport for ITER [45,46,47], but only SRO experiments will allow definitive conclusions to be drawn regarding the need for an ICH upgrade from 10 to 20 MW in the DT phases. IM studies have been performed on WEST, indicating that ICH-induced temperature anisotropy and poloidal asymmetries of electrostatic potential also have an effect on W transport: the combination of the METIS transport solver, EVE/AQL for ICH [48], QuaLiKiz for turbulent transport [49], and FACIT for neoclassical transport [50] shows that core W peaking is increased/decreased with ICH at low/high plasma rotation respectively [51]. Equivalent modelling should be carried out for ITER to quantify the effect of ICH-induced asymmetries on the W transport for ITER scenarios.
Since the new baseline relies more heavily on ECH, the operational conditions of the EC system have been reviewed in detail [52], supported by models from the H&CD IMAS workflow [53]. A study has been carried out with the TORBEAM ray-tracing code for ECH [54] to propose an optimal design for the second Equatorial Launcher (EL), needed to inject an extra 20 MW into the plasma, and intended to be non-steerable. Combined with scenario modelling carried out with ASTRA [55] and JINTRAC, the initial assessment recommends that the 2nd EL should aim to deposit power within the radial location $\rho = [0.1 - 0.45]$ to avoid strong local current drive peaks, in particular in conjunction with NBI.

3.2.2. Modelling NBI for DT-1 and DT-2 phases

From DT-1, the NBI system will operate with a nominal power of 33 MW, corresponding to 870 keV energy for H beams (in DT-1) and 1 MeV energy for D beams (in DT-1 and DT-2). One operational constraint is the enhanced NBI shine-through losses at low n_e, especially with H-NBI. A thorough analysis has been carried out to assess the shine-through losses and to choose the appropriate beam power and energy for all operational conditions of the new baseline [56]. These losses are found to be higher with H beams than with D beams, and equivalent in H, D and DT plasmas. They can be reduced by lowering the beam energy. Due to the perveance matching criteria between the beam power and energy for the ITER NBI system (which ensures that the beamlets do not diverge or over-focus), $P_{NBI} \sim E_{NBI}^{2.5}$, reducing the beam energy implies reducing the applied NBI power, and IRP scenarios have to be adjusted accordingly. The Neutral Beam Test Facility Research Plan [57] aims first to demonstrate NBI H 870 keV beams and then D 1 MeV beams. Depending on the development, the change from H to D will occur during DT-1 or in DT-2. ASTRA and JINTRAC modelling have shown no major impact when operating with H or D beams for DT-1 objectives: remaining with H beams in DT operation would reduce the fusion power by ~10 MW (i.e. alpha heating reduced by 2 MW), due to the lack of DT reactions between D beam and thermal T ions, and to the ~1% H dilution. This small power reduction could be compensated with additional RF power [58]. For DT-2 it is necessary to operate with D beams since both NB current drive and increased dilution have a larger impact on Q=5 steady-state operation.

3.2.3. Modelling H&CD towards long pulse operation

For pulses of duration ≳100 s, current diffusion plays an important role since MHD instabilities may be triggered, due e.g. to the formation of a current well which can trigger tearing modes (TM) when relaxing, requiring a robust

TM control strategy. This can be active control via local ECH/ECCD, or passive control by shaping the current profile in L-mode and early H-mode [59]. Successful passive TM control via current profile shaping for the ITER DT baseline scenario in DIII-D zero-torque ITER-like experiments could be reproduced using the CORSICA transport solver [60], together with the DCON model to calculate the ideal stability and the R-DCON model for TM [61].
Several H&CD mixes have been studied for the ITER DT baseline scenario, indicating that higher direct ion heating allows for a faster n_e rise without losing H-mode, as previously shown in [62]: transport solvers indicate that if the n_e is ramped up too quickly, with respect to the H&CD power rise, T_i never reaches 10 keV, hence the fusion power never takes off. Given that the increased n_e leads to a higher H-mode threshold, H-mode is never achieved, and the desired fusion power is never reached. The conclusion is that H&CD mixes leading to reduced direct ion heating imply a slower n_e ramp-up to access Q=10 but do not prevent it.
The operational space for steady-state operation with fully non-inductive current drive and Q=5 with 49.5 MW D-NBI and 20-30 MW ECH is derived from ASTRA simulations [63]. It was shown that such operation requires very high confinement, $H_{98} \sim 1.5 - 1.6$. Several H&CD mixes have been studied with ASTRA to assess which combination requires less confinement, indicating that applying 49.5 MA of NBI power and limited ECH is the optimal configuration. Recent core-edge-SOL-divertor integrated JINTRAC modelling has also been carried out for the 10 MA/5.3T steady-state scenarios, indicating that a minimum of Q=3-4 can be achieved even when assuming additional W sources and a confinement factor reduced to $H_{98} < 1.5$ [64]. Q=5 steady-state operation has been extensively studied in [65] using transport solvers such as METIS, ASTRA, and CORSICA combined with MHD stability analysis codes KINX [66], MISHKA [67], and DCON (embedded inside CORSICA) to investigate the ideal MHD stability of these plasmas and evaluate the margin to the high beta limit. In this context, a fully non-inductive Q~5 scenario has been developed at 10 MA using 49.5 MW NBI associated with 20 MW ECH, assuming $H_{98} = 1.6$.

3.3. Disruption loads and mitigation

Disruptions can lead to severe damage on the ITER PFCs. Due to the higher melting point of W compared to Be, these risks are considerably reduced with respect to the old baseline: they are expected to arise above ~10 MA (cf. ~7 MA with a Be FW). As a consequence, a robust mitigation strategy must be established in the path towards nominal I_p operation. Modelling activities have been necessary to assess the operational range over which loads can be characterized with acceptable risks, and where mitigation can be demonstrated. Two types of modelling have been performed:

- 2D disruption modelling originally with Be FW [68] and W divertor [69], to assess the energy deposition and material damage during unmitigated current quench of Vertical Displacement Events (VDEs) and major disruptions. For this modelling, DINA has been used to produce the relevant scenarios, together with the SMITER field line tracing tool [70] to calculate the surface power density maps on FW panels, and MEMOS-U [71] for the temperature response and associated melt motion and final surface topology on each panel. To minimize the risk of divertor water leaks due to RE impact and to protect it from plasma loads, in the SRO phase, disruptions will be directed upwards such that disruption and RE energies are deposited on the inertially-cooled FW. Axisymmetric modelling with JOREK [72] has shown that the in-vessel VS coils will be capable of directing the plasma upwards if these coils are energized some 10's of milliseconds before the thermal quench [1].
- JOREK 3D non-linear MHD modelling of unmitigated disruptions shows that the melting of a FW W from an unmitigated 15 MA current quench at highest magnetic energy occurs in very localised areas [73].

For advanced 3D modelling of disruptions, a newly developed IM workflow to generate virtual magnetic diagnostic signals was used to extract the disruption precursor signal from JOREK simulations of a radiative edge collapse [78]. The workflow simulates the disruption precursors (e.g. here the magnetic perturbations induced by the radiative collapse, with the associated magnetic signals), the disruption itself (i.e. the fast loss of thermal and magnetic energy), and its consequences (i.e. the heat loads on the FW, electro-magnetic forces, and RE-induced damage). The workflow has been applied to disruption studies in SRO 2 MA limiter plasmas, indicating that the temperature should stay marginally below the melt limits of the temporary FW in the start-up areas.
For the initial re-baseline studies, a DINA-Geant4-MEMOS-U workflow was used to assess the FW RE damage. This workflow has recently been upgraded to a DINA/JOREK-Geant4-MEMENTO workflow [74], where DINA or JOREK predicts the RE loading, Geant4 [75] simulates the RE volumetric energy deposition, and MEMENTO deduces the heat transfer to the FW. This modelling has been the driver for the decision to thicken the ITER FW W armour from 6 to 12 mm in some specific areas [6].
The mitigation strategy for RE beams is the pre-thermal-quench densification with H such that high energy electrons thermalize before the electric field exceeds the RE generation threshold (i.e. hot tail seed suppression). Recent RE modelling during both thermal and current quench phases with the DREAM code [76] has shown that

shattered pellet injection of H and Ne can lead to acceptable RE currents, except for DT plasmas at 15 MA where RE currents are too high, due to the T β-decay and Compton scattering of photons from the activated wall [77]. These results motivated the commissioning strategy introduced into the IRP to increase the T concentration stepwise from 9% to nearly 90% in the early DT phase to limit the risks to the machine while going to higher I_p.

4. CONCLUSION

A very substantial IM effort has been undertaken in support of the new re-baseline. IM tools are consistently developed to improve and refine the modelling, striving towards achieving self-consistency for physics processes taking place from the wall to the plasma core. Many of the modelling tools and assumptions have been successfully applied to present experiments, providing a validation of the models. Still, significant improvements are required to refine ITER predictions, such as extending models to higher fidelity and ensuring self-consistent plasma parameters and assumptions across all modelling codes applied. Other IM tools are currently under development, such as the ITER Pulse Design Simulator which is vital in support of future ITER operation. The development of these tools requires the involvement of the international fusion community, through the sharing of state-of-the-art models optimised for high fidelity or fast plasma simulations. Such code sharing is facilitated when the models are made publicly available for worldwide contributions by fusion experts, which is the drive for the new open-source software campaign recently launched by IO.

ACKNOWLEDGEMENTS

The views and opinions expressed herein do not necessarily reflect those of the ITER Organization. This work was performed in part under the auspices of the ITER Scientist Fellow Network.

REFERENCES

[1] A Loarte et al 2025 Plasma Phys. Cont. Fusion 67 065023
[2] S.W. Yoon et al, this conference
[3] F. Imbeaux et al, 2015 Nucl. Fusion 55 123006
[4] P. Barabaschi et al, this conference
[5] R.A. Pitts et al, 2025, Nucl. Mat. and Energy 42 101854
[6] A. Loarte et al, this conference
[7] D. Fajardo et al 2025 Plasma Phys. Cont. Fusion 67 015020
[8] C. Bourdelle, Plasma Phys. Cont. Fusion 67 (2025) 043001
[9] M. Romanelli et al., Plasma Fusion Res. 9 (2014) 3403023
[10] S.H. Kim et al, this conference
[11] X. Bonnin et al, Plasma Fusion Res. 11 (2016)
[12] S. Wiesen et al., J. Nucl. Mater. 463 (2015)
[13] R. Simonini et al, 1994 Contrib. Plasma Phys. 34 368
[14] D. Reiter 1992 J. Nucl. Mater. 196-198 80
[15] R.R. Khayrutdinov and V.E. Lukash, JPC 107 (1993) 106
[16] G. Cenacchi, A. Taroni 1988 JET-IR(88)03
[17] L. Lauro-Taroni et al 1994 21st EPS Conf. vol 18B p 102
[18] G.M. Staebler et al 2016 Phys. Plasmas 23 062518
[19] E.A Belli, J Candy 2012 Plasma Phys. Cont. Fus. 54 015015
[20] F. Köchl et al, 9th AAPPS-DPP (2025) Fukuoka
[21] D. Fajardo et al 2024 Nucl. Fusion 64 104001
[22] S. Di Genova et al 2024 Nucl. Fusion 64 126049
[23] Y. Zhang et al 2025 Nucl. Fusion 65 056035
[24] D. Farina, 2007 Fusion Sci. Technol. 52 154
[25] P. Maget et al 2022 Plasma Phys. Control. Fus. 64 045016
[26] J.P. Gunn et al 2017 Nucl. Fusion 57 046025
[27] K. Schmid et al, 2015 J. Nucl. Mater. 463 66
[28] K. Schmid and T. Wauters, Nuc. Mat. En. 41 (2024) 101789
[29] J. Garcia et al Phys. Plasmas 29, 032505 (2022)
[30] A.R. Field et al 2023 Nucl. Fusion 63 016028
[31] E. Fransson et al, Phys. Plasmas 29, 112305 (2022)
[32] V. Parail et al 2009 Nucl. Fusion 49 075030
[33] R. Dux et al, Journal of Nuc. Mat. 390–391 (2009) 858–863
[34] A. Huber et al, Nuclear Mat. and Energy 25 (2020) 100859
[35] A.R. Polevoi et al 2018 Nucl. Fusion 58 056020
[36] R. Dux et al, Nuc. Materials and Energy 12 (2017) 28–35
[37] D. Van Vugt et al, Phys. Plasmas 26, 042508 (2019)
[38] Y.Q. Liu et al, 2000 Phys. Plasmas 7 3681
[39] X Bai et al 2024 Plasma Phys. Control. Fusion 66 055017
[40] S.Q. Korving et al, Phys. Plasmas 31, 052504 (2024)
[41] Y. R. Martin et al 2008 J. Phys.: Conf. Ser. 123 012033
[42] A. Kallenbach et al 2009 Nucl. Fusion 49 045007
[43] E. Joffrin et al 2014 Nucl. Fusion 54 013011
[44] C. Angioni et al 2017 Nucl. Fusion 57 056015
[45] W. Helou et al 2023 Proc. 29th IAEA Fus. Energy Conf.
[46] L. Colas et al 2024 Proc. 26th PSI Conf. 42 101831
[47] V. Bobkov et al 2024 Proc. 26th PSI Conf. 41 101742
[48] R. Dumont, Nuclear Fusion 49 (2009) 075033
[49] C. Bourdelle et al., Phys. Plasmas 14, 112501 (2007)
[50] P. Maget et al, Plasma Phys. & Cont. Fus. 62 (2020) 105001
[51] P. Maget et al 2023 Plasma Phys. Control. Fus. 65 125009
[52] M. Schneider et al, 2025, 25th Conf. RF Power in Plasmas
[53] M. Schneider et al, 2021, Nucl. Fusion 61 126058
[54] E. Poli et al, 2018, Comp. Phys. Comm. 225, 36
[55] GV Pereverzev, PN Yushmanov 2002, IPP-Report IPP 5/98
[56] P. Vincenzi et al, 2025, Nucl. Fusion 65 036009
[57] D. Marcuzzi et al, this conference
[58] P. Vincenzi et al 2025 Plasma Phys. Cont. Fus. 67 045013
[59] F. Turco et al 2024 Nucl. Fusion 64 076048
[60] J.A. Crotinger et al 1997 LLNL Report UCRL-ID-126284 NTIS #PB2005-102154
[61] A.H. Glasser et al Phys. Fluids 18, 875–888 (1975)
[62] F Wagner et al 2010 Plasma Phys. Cont. Fusion 52 124044
[63] A.R. Polevoi et al 2020 Nucl. Fusion 60 096024
[64] S.H. Kim et al 2024 Proc. 2nd IAEA TM on Long-Pulse Operation of Fusion Devices (Vienna, Austria)
[65] S.H. Kim et al 2021 Nucl. Fusion 61 076004
[66] L. Degtyarev et al 1997 Comput. Phys. Commun. 103 10
[67] Mikhailovskii A.B. et al. 1997 Plasma Phys. Rep. 23 844
[68] J. Coburn et al 2022 Nucl. Fusion 62 016001
[69] L. Chen et al 2022 Proc. 25th PSI (Jeju, Korea)
[70] L. Kos, et al. Fus. Eng. and Design 146 (2019) 1796–1800
[71] E Thorén et al 2021 Plasma Phys. Cont. Fusion 63 035021
[72] G.T.A. Huysmans and O. Czarny 2007 Nucl. Fusion 47 659
[73] F.J. Artola et al, this conference
[74] S. Ratynskaiaa et al, submitted to Plasma Physics and Controlled Fusion, http://arxiv.org/abs/2509.20261
[75] J. Allison et al., Nuc. Inst.. Meth. Phys. Res. A835:186 2016
[76] M. Hoppe et al, Comp. Phys. Comm. 268 (2021) 108098
[77] O. Vallhagen et al 2024 Nucl. Fusion 64 086033
[78] N. Schwarz et al, 2025 51st EPS Conf. on Plasma Physics